A&A 401, 625–630 (2003)
DOI: 10.1051/0004-6361:20021871

Astronomy & Astrophysics

Point X-ray sources in the SNR G 315.4−2.30 (MSH 14−63, RCW 86)

V. V. Gvaramadze[1,2,3⋆] and A. A. Vikhlinin[4]

[1] Sternberg Astronomical Institute, Moscow State University, Universitetskij Pr. 13, Moscow 119992, Russia
[2] E.K.Kharadze Abastumani Astrophysical Observatory, Georgian Academy of Sciences, A.Kazbegi ave. 2-a, Tbilisi 380060, Georgia
[3] Abdus Salam International Centre for Theoretical Physics, Strada Costiera 11, PO Box 586, 34100 Trieste, Italy
[4] Space Research Institute, Russian Academy of Sciences, Profsoyuznaya 84/32, Moscow 117997, Russia

Received 1 August 2002 / Accepted 28 October 2002

Abstract. We report the results of a search for a point X-ray source (stellar remnant) in the southwest protrusion of the supernova remnant G 315.4−2.30 (MSH 14−63, RCW 86) using the archival data of the *Chandra X-ray Observatory*. The search was motivated by a hypothesis that G 315.4−2.30 is the result of an off-centered cavity supernova explosion of a moving massive star, which ended its evolution just near the edge of the main-sequence wind-driven bubble. This hypothesis implies that the southwest protrusion in G 315.4−2.30 is the remainder of a pre-existing bow shock-like structure created by the interaction of the supernova progenitor's wind with the interstellar medium and that the actual location of the supernova blast center is near the center of this hemispherical structure. We have discovered two point X-ray sources in the "proper" place. One of the sources has an optical counterpart with the photographic magnitude 13.38 ± 0.40, while the spectrum of the source can be fitted with an optically thin plasma model. We interpret this source as a foreground active star of late spectral type. The second source has no optical counterpart to a limiting magnitude ∼21. The spectrum of this source can be fitted almost equally well with several simple models (power law: photon index = 1.87; two-temperature blackbody: kT_1 = 0.11 keV, R_1 = 2.34 km and kT_2 = 0.71 keV, R_2 = 0.06 km; blackbody plus power law: kT = 0.07 keV, photon index = 2.3). We interpret this source as a candidate stellar remnant (neutron star), while the photon index and non-thermal luminosity of the source (almost the same as those of the Vela pulsar and the recently discovered pulsar PSR J 0205+6449 in the supernova remnant 3C 58) suggest that it can be a young "ordinary" pulsar.

Key words. stars: neutron – ISM: bubbles – ISM: individual objects: G 315.4−2.30 (MSH 14−63, RCW 86) – ISM: supernova remnants – X-ray: stars

1. Introduction

G 315.4−2.30 (MSH 14−63, RCW 86) is a bright (in both radio and X-ray) shell-like supernova remnant (SNR) with a peculiar protrusion to the southwest (e.g. Dickel et al. 2001; Vink et al. 1997). This protrusion encompasses a bright hemispherical optical nebula (Rodger et al. 1960, Smith 1997; see also Fig. 3). The characteristic angular size of the SNR is about 40′, that at a distance to the remnant of 2.8 kpc (Rosado et al. 1996) corresponds to ≃32 pc. The radius of the optical nebula is ≃2′ (or ≃1.6 pc). A collection of observational data points to the young age (few thousand years) of the SNR (see e.g. Dickel et al. 2001).

Vink et al. (1997) put forward the idea that the SNR G 315.4−2.30 is the result of a supernova (SN) explosion inside a pre-existing wind-driven cavity (see also Dickel et al. 2001; Vink et al. 2002) and noted that the elongated shape of the SNR resembles that of a wind-driven cavity created by a *moving* massive star (see Weaver et al. 1977 and Brighenti & D'Ercole 1994 for details). On the other hand, it is believed that the origin of the southwest protrusion is due to the interaction of the SN blast wave with a density enhancement in the ambient interstellar medium. However, as was correctly noted by Dickel et al. (2001), the density enhancement (e.g. a high-density cloud) should result in a concave dent in the shell, not in a protrusion. Dickel et al. (2001) also suggested that this protrusion "is perhaps the key to what is going on".

We agree with the idea that G 315.4−2.30 is a diffuse remnant of an off-centered cavity SN explosion and supplement this idea by the suggestion that the massive SN progenitor star exploded near the edge of the main-sequence bubble. This suggestion implies that the southwest protrusion is the remainder of a bow shock-like structure created in the interstellar medium

Send offprint requests to: V. V. Gvaramadze,
e-mail: vgvaram@sai.msu.ru
⋆ *Address for correspondence*: Krasin str. 19, ap. 81, Moscow 123056, Russia.

by the post-main-sequence winds (see Sect. 4 and Gvaramadze 2002; cf. Wang et al. 1993) and that the SN exploded near the center of this hemispherical structure. Given the youth of the SNR and assuming a reasonable kick velocity for the stellar remnant, one can expect that the stellar remnant should still be within the protrusion. Motivated by these arguments, Gvaramadze (2002) searched for a possible compact X-ray source to the southwest of G 315.4−2.30 using the *ROSAT* archival data, but the moderate spatial resolution of the *ROSAT* PSPC precluded detection of point sources against the bright background emission of the SNR's shell.

In this paper we report the discovery of two point X-ray sources near the center of the hemispherical optical nebula using the archival Advanced CCD Imaging Spectrometer (ACIS) data of the *Chandra X-Ray Observatory*. We interpret one of the sources as a foreground active star of late spectral type, and the second one as a candidate stellar remnant (neutron star).

Note that Vink et al. (2000) also reported the discovery of a point X-ray source in the southwest half of G 315.4−2.30, at about 7′ from the geometrical center of the SNR. We recall that Vink et al. (1997) suggested that the SN blast wave in this SNR takes on the shape of the pre-existing elongated cavity (created by the stellar wind of the moving SN progenitor star). However, the initially spherical shape of the wind-driven cavity could be significantly affected by the stellar motion only if the massive star reaches the edge of the cavity and the stellar wind starts to interact directly with the ambient interstellar medium (e.g. Weaver et al. 1977); this implies that the SN explodes near the edge of the future (young) SNR (see Sect. 4). However, the source discovered by Vink et al. (2000) is located too far from the edge of G 315.4−2.30. Moreover, the spectral characteristics of the source and the presence of a possible optical counterpart suggest that it is an active star rather than the stellar remnant associated with the SNR (Vink et al. 2000; see also Sect. 3.1).

2. Point X-ray sources

2.1. X-ray images

Figure 1 shows the *Chandra* (0.7−2 keV) image of the highly structured southwest corner of the SNR G 315.4−2.30. Two point X-ray sources are clearly visible at the northwest of the image at $\alpha_{2000} = 14^{\rm h}40^{\rm m}31\overset{\rm s}{.}33, \delta_{2000} = -62°38'22\overset{''}{.}8$ and $\alpha_{2000} = 14^{\rm h}40^{\rm m}31\overset{\rm s}{.}05, \delta_{2000} = -62°38'16\overset{''}{.}9$. For both sources we measured a *FWHM* of $1\overset{''}{.}1$, which is consistent with the *Chandra* point spread function at the off-axis angle $2\overset{'}{.}5$. Figure 2 shows a close-up of the region around the sources, labelled S (southern source) and N (northern source).

2.2. Optical images

Figure 3 shows the image of the hemispherical optical nebula to the southwest of the SNR G 315.4−2.30 from the Digital Sky Survey (DSS-2, red plates). Figure 4 shows an enlarged view of the region around the point X-ray sources. The source S is in good positional agreement with a point-like object immersed in a diffuse optical filament. This object is indicated in the HST Guide Star Catalog as non-stellar, with a photographic

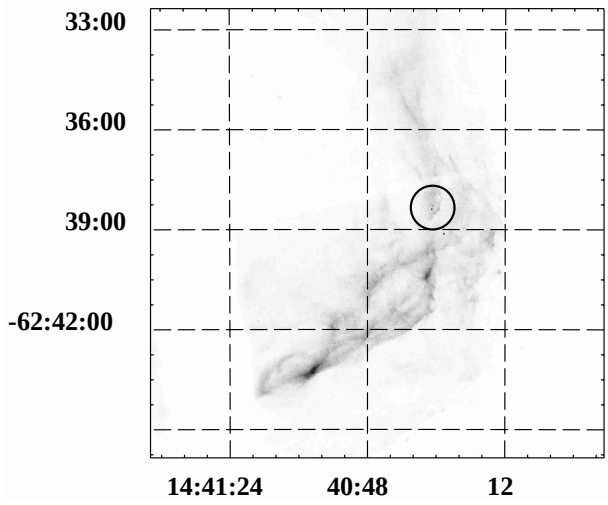

Fig. 1. *Chandra* image of the southwest region of the SNR G 315.4−2.30. Both X-ray sources are surrounded by a circle. North is up and east is to the left.

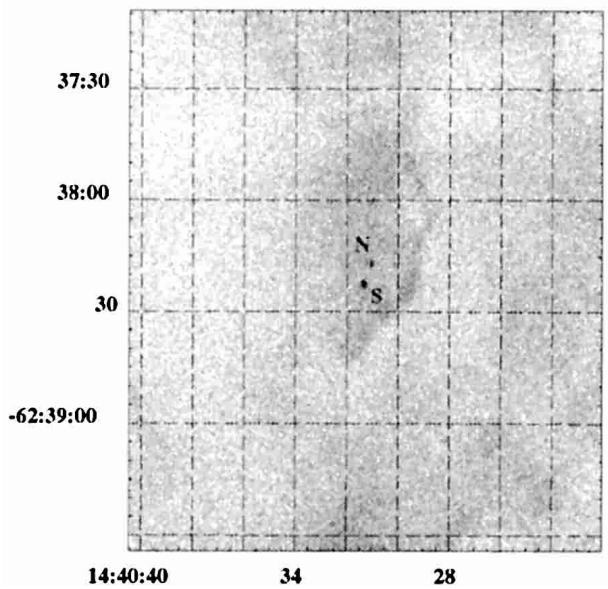

Fig. 2. The enlarged view of the region around the point X-ray sources, labelled S (southern) and N (northern).

magnitude of 13.38±0.40. We believe, however, that it was misclassified due to the effect of the background diffuse emission and in fact it is a star. The source N has no optical counterpart to a limiting magnitude ∼21.

2.3. Spectral analysis

The spectra of the point sources were extracted from circular regions with radii of 1.5 arcsec. The background spectrum was taken from a circle with a radius of 4.5 arcsec at 6.5 arcsec northeast of the point sources. The PSF model shows that the fraction of the source flux in the background region is negligible. The spectral modeling was performed in the 0.5−10 keV energy range using the XSPEC spectra fitting package. The estimates of the interstellar absorption, $N_{\rm H}$,

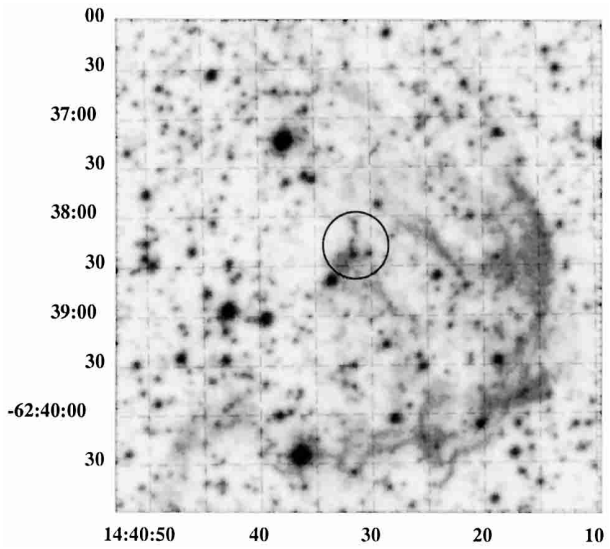

Fig. 3. The DSS-2 image of the optical nebula southwest of the SNR G 315.4−2.30. The position of both point X-ray sources is surrounded by a circle.

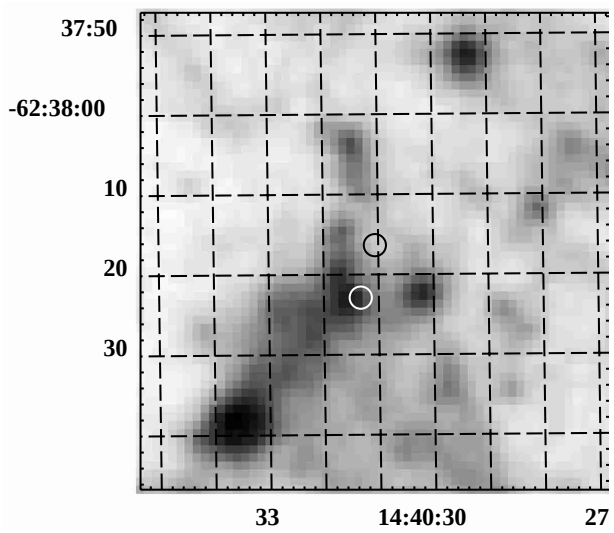

Fig. 4. The enlarged DSS-2 image of the region around the point X-ray sources. The circles are centered at the position of X-ray sources.

towards G 315.4−2.30 are quite uncertain (cf. e.g. Vink et al. 1997 with Vink et al. 2002), so the spectra were fitted with $N_{\rm H}$ as a free parameter. In one case, however, we used the fixed value of $N_{\rm H}$ (see below).

The spectrum of the source S is shown in Fig. 5; the solid line represents the best fit optically thin plasma model, with a temperature = 0.69 ± 0.05 keV, abundance = 0.07 ± 0.02, $N_{\rm H} = (1.2 \pm 0.3) \times 10^{21}\,{\rm cm}^{-2}$, luminosity (in the 0.5–10 keV energy range) $\simeq 2.8 \times 10^{31}\,{\rm erg\,s}^{-1}$, and χ^2/d.o.f. = 21.6/25. The blackbody or power law models give unacceptable fits.

The spectrum of the source N (shown in Fig. 6) can be fitted almost equally well with a power law (PL), two-temperature blackbody (BB+BB), or blackbody plus power law (BB+PL) models. A simple BB model gives unacceptable fits. The best fit spectrum predicted by the BB+PL model is shown in Fig. 6 by the solid line.

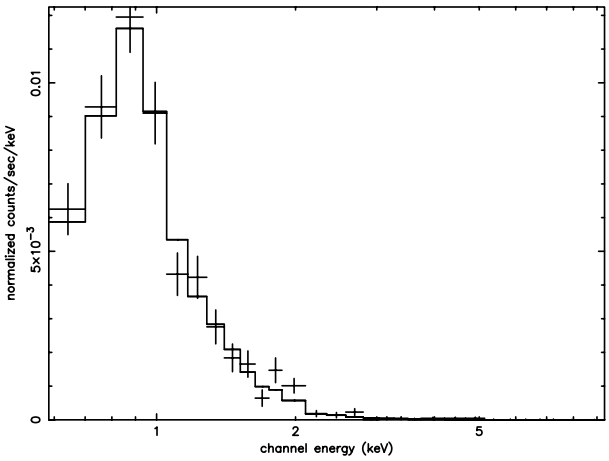

Fig. 5. The background-subtracted *Chandra* ACIS spectrum from the source S. The solid line represents the best fit optically thin plasma model.

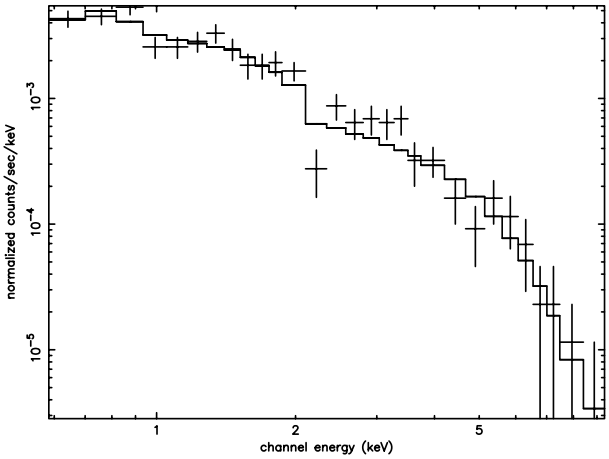

Fig. 6. The background-subtracted *Chandra* ACIS spectrum from the source N. The solid line corresponds to the best fit blackbody plus power law model.

We note that the best fit PL model requires $N_{\rm H} = 0$ (we consider this fact as an indication of the galactic origin of the source N), although models with $N_{\rm H}$ up to $1.5 \times 10^{21}\,{\rm cm}^{-2}$ (presented in Table 1) also give acceptable fits.

The results of a spectral analysis for the source N are summarized in Table 1.

3. Discussion

3.1. Source S

The soft X-ray spectrum of the source S and the existence of the candidate optical counterpart strongly suggest that this source is an active star. Assuming that S is indeed a star and given the observed X-ray to optical flux ratio, one can exclude the possibility that this star is of the OB-type. Therefore it cannot be a member of a group of OB stars located in the direction of G 315.4−2.30 nearly at the same distance as the SNR (Westerlund 1966). Most likely the source S is a foreground active star of late spectral type. A follow-up study of this object could clarify its nature.

Table 1. Spectral fits to the point X-ray source N.

Model	Photon index	Temperature, keV	$N_{\rm H}$, 10^{21} cm^{-2}	Luminosity, 10^{32} erg s^{-1}	χ^2 /d.o.f.[a]
PL	1.87 ± 0.09		1.5 (fixed)	0.44 (0.5−10 keV)	51.5/27
B+B		0.11 ± 0.03	4.3 ± 1.8	1.32 (bolometric)	47.3/25
		0.71 ± 0.05		0.35 (bolometric)	
BB+PL		0.070 ± 0.003	9.2 ± 3.4	112 (bolometric)	38.9/25
	2.31 ± 0.30			0.67 (0.5−10 keV)	

[a] Note that a single point near the Chandra mirror edge contributes ≃ 10 to the χ^2 in all cases.

Note that the point X-ray source discovered by Vink et al. (2000) has much in common with the source S. The spectra of both sources are soft and could be fitted with the optically thin plasma model with depleted abundances (typical of late-type stars; e.g. Giampapa et al. 1996). Both sources have candidate optical counterparts with almost the same photographic magnitudes. In both cases the X-ray to optical flux ratios suggest that the optical objects are late-type stars. Evidence for long-term variability of the former source (Vink et al. 2000) also suggest that it is an active star.

3.2. Source N

The spectral characteristics of the source N coupled with the absence of an optical counterpart allow us to consider it as a candidate stellar remnant. We now discuss this possibility.

3.2.1. Power law model

The PL fit of the spectrum (with the photon index typical of pulsars) suggest that the source N can be an active (rotation-powered) neutron star. Assuming that N is a pulsar[1] and using the empirical relationships between the non-thermal X-ray and spin-down luminosities of pulsars (e.g. Becker & Trümper 1995; Possenti et al. 2002), one can estimate the latter, $\dot{E} \sim 10^{35}\, d_{2.8}^2$ erg s^{-1}, where $d_{2.8}$ is the distance to the SNR in units of 2.8 kpc.

The inferred low spin-down luminosity can be considered as an argument against the possibility that the source N is a young fast-rotating pulsar with a standard magnetic field (10^{11}–10^{13} G). Therefore N can be either a young pulsar born with a low surface magnetic field (e.g. Blandford et al. 1983; Urpin et al. 1986) and/or a large rotation period (e.g. Spruit & Phinney 1998) or an aged pulsar with a decaying magnetic field. The first possibility would deserve detailed consideration if a candidate period of 12 ms found for the central X-ray source in Cas A (Murray et al. 2002a) is confirmed by an independent timing analysis. The second one implies that N is an old pulsar (of an arbitrary age) projected by chance on the SNR G 315.4−2.30.

Note, however, that the above-mentioned empirical relationships are quite uncertain and should be used with caution. For example, the 267 ms radio pulsar PSR B 1853+01 associated with the SNR W 44 (Wolszczan et al. 1991) has almost the same spin-down luminosity ($\simeq 4\times10^{35}$ erg s^{-1}) as that derived above for the source N, while the characteristic age of the pulsar ($\simeq 2\times10^4$ yr; consistent with a range of ages derived for W 44 using the standard Sedov-Taylor model, see Smith et al. 1985) points to its relative youth. On the other hand, the pulsar PSR B 1853+01 could be much older if its high spin-down rate ($\dot{P} \simeq 0.2\times10^{-12}$ s s^{-1}) is connected to the interaction between the pulsar's magnetosphere and the dense circumstellar matter[2] (cf. Gvaramadze 2001). The age of W 44 also could be much greater if the origin of this mixed-morphology SNR is due to the cavity SN explosion (cf. Gvaramadze 2002).

The uncertainties inherent to the empirical relationships are more obvious in the case of the pulsar PSR J 0205+6449, recently discovered in the SNR 3C 58. The spin-down luminosity of this young (characteristic age ≃5400 yr) pulsar is 2.6×10^{37} erg s^{-1} (Murray et al. 2002b), while its (non-thermal; see Slane et al. 2002) X-ray luminosity is $\simeq 2.1\times10^{32}\, d_{2.6}^2$ erg s^{-1}, i.e. about two orders of magnitude less than that predicted by the empirical relationships. The disparity between the predicted and observed non-thermal luminosities is even higher in the case of another young pulsar – the Vela pulsar (Pavlov et al. 2001). Note that the photon indices and non-thermal luminosities of these two pulsars are almost the same as those predicted for the source N by the PL (or BB+PL) model, while their characteristic ages are of the same order of magnitude as the age of the SNR G 315.4−2.30 inferred in Sect. 4. Therefore one cannot exclude that the source N is a young pulsar with "ordinary" parameters. This should be tested observationally.

3.2.2. Two-temperature blackbody model

In the two-temperature blackbody model, the origin of the soft component can be attributed to the cooling surface of a neutron star, while the hard component to the polar caps heated by the backflow of relativistic particles (e.g. Wang et al. 1998).

The best-fit BB+BB model yields the temperature of the soft component of 0.11 keV and the effective radius of 2.3 km. The inferred temperature is somewhat larger than that predicted by standard cooling models (e.g. Page 1998), while the radius is significantly smaller than the radius of the neutron star. In principle, one can expect that the use of realistic neutron star atmosphere models (e.g. Pavlov et al. 1995) would adjust

[1] The 3.2 s individual exposure time of the ACIS instrument makes the search for short pulsations impossible.

[2] The large dispersion measure variations inherent to this pulsar (Jacoby & Wolszczan 1999) could be considered as an indirect support of this suggestion.

these parameters to acceptable values. But the interpretation of the hard component is more problematic. The effective polar cap area inferred from the best-fit BB+BB model ($\sim 10^8$ cm^{-2}) is too small and the observed temperature is too large to be consistent with models for heating of polar caps (e.g. Wang et al. 1998 and references therein). Therefore we consider this model as unplausible and suggest that at least at high energies the X-ray emission of the source N is non-thermal.

3.2.3. Blackbody plus power law model

The use of the BB+PL model assumes that the soft X-ray emission comes from the entire surface of a cooling neutron star or from some smaller hot areas, while the hard X-rays are due to the non-thermal magnetospheric emission.

The best fit BB+PL model shows that the spectrum of the source N is dominated by the non-thermal emission at energies >1 keV, and suggests the existence of a soft thermal component. However, the unknown interstellar absorption and uncertainties due to the time-dependent decrease in ACIS low-energy quantum efficiency make the estimates of the flux and bolometric luminosity of the BB component unconstrained. The best fit model with $N_{\rm H}$ as a free parameter (see Table 1) requires large interstellar absorption and consequent large bolometric luminosity. Although the large absorption, in principle, is consistent with values derived by Vink et al. (2002) for the SNR G 315.4−2.30, the large inferred bolometric luminosity implies an uncomfortably large effective radius of ≃60 km. The normalization of the BB component, however, is plausible for lower values of $N_{\rm H}$. A more detailed consideration of this problem will be possible only with updated *Chandra* calibration at low energies. Note that dense clumps of circumstellar matter (the natural products of interaction between post-main-sequence winds of the SN progenitor star; e.g. Gvaramadze 2001 and references therein; see also Sect. 4) could add a significant contribution to the neutral hydrogen absorption towards the source N, as well as possibly causing the enhanced absorption towards the central compact source in Cas A (required by some model fits of its spectrum; e.g. Murray et al. 2002a).

Note also that at present we cannot definitively confirm or reject the existence of a soft BB component. Therefore we consider the PL model with a reasonable value of $N_{\rm H}$ as a good approximation for the spectrum of the source N. The follow-up multiwavelength observations of this source, including the search for pulsed emission, long term variability, and radio, optical or γ-ray counterparts, may provide crucial information for an understanding of its nature and therefore are highly desirable.

4. SNR G 315.4−2.30

We now briefly discuss a scenario for the origin of the SNR G 315.4−2.30 (a more detailed description will be presented elsewhere). We note that our scenario has much in common with the model proposed by Wang et al. (1993) to explain the origin of large-scale structures around the SN 1987A, and suggest that G 315.4−2.30 is an older version of the latter.

We believe that the SNR G 315.4−2.30 is the result of a cavity SN explosion of a moving massive star, which after the main-sequence (MS) phase (lasting $\sim 10^7$ yr) has evolved through the red supergiant (RSG) phase ($\sim 10^6$ yr), and then experienced a short ($\sim 10^4$ yr) "blue loop" (i.e. the zero-age MS mass of the star was 15−20 $M_\odot$). During the MS phase the stellar wind (with the mechanical luminosity, L, of $\sim 10^{35}$ erg s^{-1}) blows a large-scale bubble in the interstellar medium. The bubble eventually stalls at radius $R_{\rm st} \sim 12(L_{35}/n)^{1/2}$ pc in time $t_{\rm st} \sim 10^6 (L_{35}/n)^{1/2}$ yr, where $L_{35} = L/10^{35}$ erg s^{-1} and n is the number density of the interstellar gas. The current radius of SNR G 315.4−2.30 is ≃16 pc. The motion of that star causes it to cross the stalled bubble and start to interact directly with the unperturbed interstellar gas. This happens at time $t_{\rm cr} \simeq R_{\rm st}/v_\star = 2.4 \times 10^6 (L_{35}/n)^{1/2} v_{\star,5}^{-1}$ yr, where $v_{\star,5}$ is the stellar velocity in units of 5 km s^{-1}. The time is in agreement with the duration of the MS phase if $v_\star \simeq 1$ km s^{-1}. In this case the SN progenitor star enters in the RSG phase while it is near the edge of the MS bubble. During the relatively short RSG phase, the star loses most (two thirds) of its initial mass in the form of a dense, slow wind. The interaction of the RSG wind with the interstellar medium results in the origin of a bow shock-like structure with a characteristic radius, r, determined by the relationship: $\dot{M}_{\rm RSG} v_{\rm RSG}/4\pi r^2 \simeq n(2kT + m_{\rm H} v_\star^2)$, where $\dot{M}_{\rm RSG}$ and $v_{\rm RSG}$ are, correspondingly, the mass-loss rate and wind velocity during the RSG phase, T is the temperature of the ambient interstellar medium, k is the Boltzmann constant, and $m_{\rm H}$ is the mass of a hydrogen atom. For $n \simeq 1$ cm^{-3} (Smith 1997, Ghavamian et al. 2001), $\dot{M}_{\rm RSG} = 10^{-5} M_\odot$ yr^{-1}, $v_{\rm RSG} = 10$ km s^{-1}, $T = 8000$ K, and $v_\star = 1$ km s^{-1}, one has $r \simeq 1.5$ pc. This value is in a comfortable agreement with the radius of the hemispherical optical nebula in the southwest of G 315.4−2.30 (≃1.6 pc).

About $\sim 10^4$ yr before the SN explosion the progenitor star becomes a blue supergiant whose fast wind sweeps the material of the RSG wind. We speculate that at the moment of SN explosion the blue supergiant wind was trapped in the southwest direction by the dense material of the bow shock-like structure, while in the opposite direction it was able to break out in the low-density MS bubble, so that the SN explodes inside a "hollow" hemispherical structure open towards the MS bubble.

The SN blast wave expands almost freely across the low-density MS bubble (for the explosion energy of 10^{51} erg and mass of the SN ejecta of ≃3.5 $M_\odot$, the expansion velocity of the blast wave is $v_{\rm bl} \simeq 5000$ km s^{-1}) and reaches the northeast edge of the bubble after $\sim 4.7 \times 10^3$ yr. The density jump at the edge of the bubble results in the abrupt deceleration of the blast wave to a velocity of $\sim(\beta n_{\rm b}/n)^{1/2} v_{\rm bl} \sim 600$−800 km s^{-1} (the values derived from studies of Balmer-dominated filaments encircling the SNR G 315.4−2.30; Long & Blair 1990 and Smith 1997), where $\beta \simeq 5$ (e.g. Sgro 1975). This deceleration implies a density jump of a factor of ≃200−300 or a number density of the MS bubble gas $n_{\rm b} \simeq 0.003$−0.005 cm^{-3}, i.e. a reasonable value given the mass lost during the MS phase is $\sim 0.5\ M_\odot$.

In the southwest direction, however, the expansion of the SN blast wave is hampered by the dense hemispherical circumstellar shell. The shocked remainder of this shell are now seen as the bright southwest protrusion (shown in Fig. 3).

The existence of radiative filaments in this corner of the SNR implies that the blast wave slows down to the velocity of $\simeq 100\,\mathrm{km\,s^{-1}}$, that in its turn implies the density contrast of $\sim 15\,000$. For $n_\mathrm{b} = 0.003\,\mathrm{cm^{-3}}$, one has the number density of the circumstellar material of $\sim 50\,\mathrm{cm^{-3}}$, i.e. in a good agreement with the density estimate derived by Leibowitz & Danziger (1983). On the other hand, the recent discovery of Balmer-dominated filaments protruding beyond the radiative arc (see Fig. 3 of Smith 1997 and Fig. 4 of Dickel et al. 2001) suggests that the SN blast wave has partially overrun the clumpy circumstellar shell (cf. Franco et al. 1991) and now propagates through the interstellar medium. We believe that this effect is responsible for the complicated appearance of the southwest corner of the SNR. For the radial extent of protrusions of $\simeq 2$ pc, and assuming that their mean expansion velocity is $\sim 700\,\mathrm{km\,s^{-1}}$, one has that the blowouts occured $\sim 3 \times 10^3$ yr ago.

5. Conclusion

We have analyzed the archival *Chandra X-Ray Observatory* data on G 315.4−2.30 to search for a stellar remnant in the southwest corner of this SNR. The search was motivated by the hypothesis that the SNR G 315.4−2.30 is the result of an off-centered cavity SN explosion of a moving massive star, which ends its evolution just near the edge of the main-sequence wind-driven bubble. This hypothesis implies that the southwest protrusion in G 315.4−2.30 is the shocked material of a pre-existing circumstellar structure and that the actual location of the SN blast center is near the center of this structure. We have discovered two point X-ray sources in the "proper" place. One of the sources is interpreted as a foreground active star of late spectral type, while the second one as a candidate neutron star (perhaps a young "ordinary" pulsar). The follow-up observations of these sources will help us to understand their nature and thereby to test the hypothesis of the origin of the SNR G 315.4−2.30.

Acknowledgements. We are grateful to J. R. Dickel (the referee) for useful suggestions and comments.

References

Becker, W., & Trümper, J. 1997, A&A, 326, 682
Blandford, R. D., Applegate, J. H., & Hernquist, L. 1983, MNRAS, 204, 1025
Brighenti, F., & D'Ercole, A. 1994, MNRAS, 270, 65
Dickel, J. R., Strom, R. G., & Milne, D. K. 2001, ApJ, 546, 447
Franco, J., Tenorio-Tagle, G., Bodenheimer, P., & Różyczka, M. 1991, PASP, 103, 803
Ghavamian, P., Raymond, J., Smith, C. R., & Hartigan, P. 2001, ApJ, 547, 995
Giampapa, M. S., Rosner, R., Kashyap, T. A., et al. 1996, ApJ, 463, 707
Gvaramadze, V. V. 2001, A&A, 374, 259
Gvaramadze, V. V. 2002, in New Visions of the X-ray Universe in the XMM-Newton and Chandra Era, ed. F. Jansen, ESA SP-488, in press [astro-ph/0208028]
Jacoby, B. A., & Wolszczan, A. 1999, in Pulsar Timing, General Relativity and the Internal Structure of Neutron Stars, ed. Z. Arzoumanian, F. Van der Hooft, & E. P. J. van den Heuvel (Koninklijke Nederlandse Akademie van Wetenschappen: Amsterdam), 157
Leibowitz, E. M., & Danziger, I. J. 1983, MNRAS, 204, 273
Long, K. S., & Blair, W. P. 1990, ApJ, 358, L13
Murray, S. S., Ransom, S. M., Juda, M., Hwang, U., & Holt, S. S. 2002a, ApJ, 566, 1039
Murray, S. S., Slane, P. O., Seward, F. D., Ranson, S. M., & Gaensler, B. M. 2002b, ApJ, 568, 226
Page, D. 1998, in The Many Faces of Neutron Stars, ed. R. Buccheri, J. van Paradijs, & M. A. Alpar (Kluwer: Dordrecht), 539
Pavlov, G. G., Shibanov, Yu. A., Zavlin, V. E., & Meyer, R. D. 1995, in The Lives of the Neutron Stars, ed. M. A. Alpar, Ü. Kiziloğlu, & J. van Paradijs (Kluwer: Dordrecht), 71
Pavlov, G. G., Zavlin, V. E., Sanwal, D., Burwitz, V., & Garmire, G. P. 2001, ApJ, 552, L129
Possenti, A., Cerutti, R., Colpi, M., & Mereghetti, S. 2002, A&A, 387, 993
Rodgers, A. W., Campbell, C. T., & Whiteoak, J. B. 1960, MNRAS, 121, 103
Rosado, M., Ambrocio-Cruz, P., Le Coarer, E., & Marcelin, M. 1996, A&A, 315, 243
Sgro, A. G. 1975, ApJ, 197, 621
Slane, P., Helfand, D. J., & Murray, S. S. 2002, ApJ, 571, L45
Smith, R. C. 1997, AJ, 114, 2664
Smith, A., Jones, L. R., Watson, M. G., et al. 1985, MNRAS, 217, 99
Spruit, H., & Phinney, E. S. 1998, Nature, 393, 139
Urpin, V. A., Levshakov, S. A., & Yakovlev, D. G. 1986, MNRAS, 219, 703
Vink, J., Kaastra, J. S., & Bleeker, J. A. M. 1997, A&A, 328, 628
Vink, J., Bocchino, F., Damiani, F., & Kaastra, J. S. 2000, A&A, 362, 711
Vink, J., Bleeker, J., Kaastra, J., van der Heyden, K., & Dickel, J. 2002, in New Visions of the X-ray Universe in the XMM-Newton and Chandra Era, ed. F. Jansen, ESA SP-488, in press [astro-ph/0112216]
Wang, L., Dyson, J. E., & Kahn, F. D. 1993, MNRAS, 261, 391
Wang, F. Y.-H., Ruderman, M., Halpern, J. P., & Zhu, T. 1998, ApJ, 498, 373
Weaver, R., McCray, R., Castor, J., & Shapiro, P. 1977, ApJ, 218, 377
Westerlund, B. E. 1966, AJ, 74, 879
Wolszczan, A., Cordes, J. M., & Dewey, R. J. 1991, ApJ, 372, L99